

Stereoselective Preparation, Structures, and Reactivities of Phosphine-Bridged Mixed-Metal Trinuclear and Pentanuclear Complexes with Tris[2-(diphenylphosphino)ethyl]phosphine

Sen-ichi Aizawa,^{*,†} Kenji Saito,[†] Tatsuya Kawamoto,[‡] and Emi Matsumoto[†]

Faculty of Engineering, Toyama University, 3190 Gofuku, Toyama 930-8555, Japan, and Department of Chemistry, Graduate School of Science, Osaka University, 1-16 Machikaneyama, Toyonaka, Osaka 560-0043, Japan

Received February 17, 2006

The phosphine-bridged linear trinuclear and pentanuclear complexes with Pd(II)–Pt(II)–Pd(II), Ni(II)–Pt(II)–Ni(II), and Rh(III)–Pd(II)–Pt(II)–Pd(II)–Rh(III) metal-ion sequences were almost quantitatively formed by the stepwise phosphine-bridging reaction of the terminal phosphino groups of tris[2-(diphenylphosphino)ethyl]phosphine (pp₃), which is the tetradentate bound ligand of the starting Pd(II) and Ni(II) complexes. The solid-state structures of the trinuclear complexes were determined by X-ray structural analyses, and the structures of the polynuclear complexes in solution were characterized by NMR spectroscopy. The trans and cis isomers of the trinuclear and pentanuclear complexes, which arise from the geometry around the Pt(II) center, were selectively obtained simply by changing the counteranion of the starting complexes: the tetrafluoroborate salts, [MX(pp₃)](BF₄) [M = Pd(II) or Ni(II), X = Cl[−] or 4-chlorothiophenolate (4-Cltp[−])], gave only the trans isomers, and the chloride salt, [PdCl(pp₃)]Cl, gave only the cis isomers. The formation of the trinuclear complex with the 4-Cltp[−] and chloro ligands, *trans*-[Pt(4-Cltp)₂{PdCl(pp₃)₂}(BF₄)₂], proceeded with exchange between the thiolato ligand in the starting Pd(II) complex, [Pd(4-Cltp)(pp₃)](BF₄), and the chloro ligands in the starting Pt(II) complex, *trans*-[PtCl₂(NCC₆H₅)₂], retaining the trans geometry around the Pt(II) center. In contrast, the formation reaction between [PdCl(pp₃)]Cl and *trans*-[PtCl₂(NCC₆H₅)₂] was accompanied by the trans-to-cis geometrical change on the Pt(II) center to give the trinuclear complex, *cis*-[PtCl₂{PdCl(pp₃)₂}Cl]₂. The mechanisms of these structural conversions during the formation reactions were elucidated by the ³¹P NMR and absorption spectral changes. The differences in the catalytic activity for the Heck reaction were discussed in connection with the bridging structures of the polynuclear complexes in the catalytic cycle.

Introduction

Cooperative effects of different metal complexes are attractive for the design of new chemical reactions. Because various phosphine complexes have been successfully used for a variety of catalytic reactions recently, deriving new cooperative catalytic effects can be one of the next goals. However, in the case where different catalysts exist independently in the reaction solution, the cooperative catalytic action may be entropically unfavorable. Therefore, if one can prepare the mixed-metal polynuclear complexes with an intended metal-ion sequence, the cooperative effect of the different metal centers of the catalysts and cocatalysts can

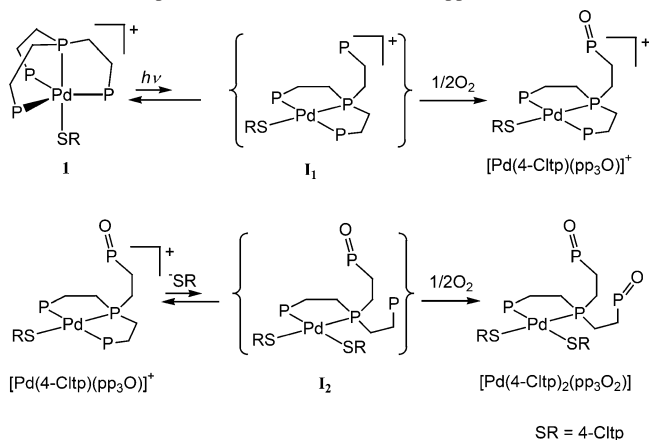
be investigated straightforward and systematically. Previously, we have found that one terminal phosphino group of the five-coordinate trigonal-bipyramidal Pd(II) complex, [Pd(4-Cltp)(pp₃)]⁺ [**1**; 4-Cltp = 4-chlorothiophenolate, pp₃ = tris[2-(diphenylphosphino)ethyl]phosphine], is selectively oxidized by photolysis and further oxidation of another terminal phosphino group proceeds quantitatively by reaction with more than an equimolar amount of 4-Cltp[−] (Scheme 1).¹ Expecting that intermediates with a dissociated terminal phosphino group (**I**₁ and **I**₂) are formed, we have designed the stepwise phosphine-bridging reaction with different metal ions instead of stepwise oxidation. Though a few phosphine-bridged complexes with two kinds of metal ions have been

* To whom correspondence should be addressed. E-mail: saizawa@eng.toyama-u.ac.jp (S.-i.A.). Phone and fax: (+81) 76 445 6980.

[†] Toyama University.

[‡] Osaka University.

(1) Aizawa, S.; Kawamoto, T.; Saito, K. *Inorg. Chim. Acta* **2004**, *357*, 2191.

Scheme 1. Stepwise Oxidation Reaction of the pp₃ Ligand in **1**

reported recently,² we have pursued synthetic studies of phosphine-bridged polynuclear complexes for the quantitative preparation of trinuclear and pentanuclear mixed-metal complexes with intended metal sequences, taking advantage of the formation of Pd(II) intermediates with a dissociated terminal phosphino group. The selective preparation of their isomers and some structural conversions during the formation reactions are also reported in this paper. Furthermore, because phosphinepalladium(II) complexes have been widely used for the C–C coupling reactions as the catalysts,³ we investigated the Heck reaction^{3b,c} by using the polynuclear and mononuclear complexes and discussed their structures in the catalytic reactions.

Experimental Section

Materials. Chloroform (Wako, infinitely pure) was dried over activated 4A molecular sieves and used as a solvent for UV–vis absorption spectral measurements. Tris[2-(diphenylphosphino)ethyl]phosphine (pp₃, Aldrich), bis[2-(diphenylphosphino)ethyl]phenylphosphine (p₃, Strem), 1,2-bis(diphenylphosphino)ethane (p₂, Kanto Chemical), 4-chlorothiophenol (H-4-Cltp, Wako), tetrakis(acetonitrile)palladium(II) tetrafluoroborate ([Pd(NCCH₃)₄](BF₄)₂, Aldrich), potassium tetrachloropalladate(II) (K₂[PdCl₄], Aldrich), *trans*-bis(benzonitrile)dichloroplatinum(II) (*trans*-[PtCl₂(NCC₆H₅)₂], Strem), dichloro-*μ*-chlorobis(pentamethylcyclopentadienyl)dirhodium(III)⁴ ([Rh₂Cl₂(*μ*-Cl)₂Cp*₂], Aldrich), silver tetrafluoroborate (AgBF₄, Wako), nickel chloride (Wako), tetra-*n*-butylammonium tetrafluoroborate (Bu₄NBF₄, Aldrich), tetra-*n*-butylammonium chloride (Bu₄NCl, Wako), iodobenzene (Kanto Chemical), styrene (Wako), tributylamine (Wako), and bis(2-butoxyethyl) ether (Wako) were used for the preparation or catalytic reactions without further purification.

Preparation of Complexes. Mononuclear Palladium(II) Complexes. [Pd(4-Cltp)(pp₃)](BF₄) [**1**(BF₄)],¹ [PdCl(pp₃)Cl] (**2**Cl),⁵ and

[PdCl(pp₃)Cl] (**3**Cl)⁵ were prepared by the reported procedures. **2**Cl was converted to **2**(BF₄) by using 1 equiv of AgBF₄ in chloroform. [PdCl₂(p₂)] (**4**) was prepared by a procedure similar to that for **3**Cl by the reaction of an aqueous solution of K₂[PdCl₄] and a chloroform solution of p₂ followed by concentration of the chloroform layer.

[NiCl(pp₃)Cl] (**5**Cl). **5**Cl was prepared by the reported procedure with some modification.⁶ To a solution containing NiCl₂ (0.115 g, 0.883 mmol) in water (20 cm³) were added a solution containing pp₃ (0.592 g, 0.883 mmol) in chloroform (20 cm³) and then ethanol (30 cm³). The resultant purple solution was stirred at 50 °C for 2 h. After the addition of water (200 cm³), the purple complex was extracted with chloroform (150 cm³). The extract was concentrated to ca. 10 cm³ and kept in a refrigerator to give purple needle crystals. Yield: 89%. Anal. Calcd for C₄₂H₄₂Cl₂NiP₄·2H₂O: C, 60.32; H, 5.54; N, 0.00. Found: C, 59.87; H, 5.57; N, 0.00.

[NiCl(pp₃)](BF₄) [**5**(BF₄)]. **5**(BF₄) was prepared by a procedure similar to that reported for **5**(AsF₆).⁷ To a solution containing NiCl₂ (0.090 g, 0.697 mmol) and Bu₄NBF₄ (0.673 g, 2.04 mmol) in ethanol (15 cm³) were added a solution containing pp₃ (0.467 g, 0.697 mmol) in chloroform (5 cm³) and then ethanol (30 cm³). The resultant reddish-purple solution was heated at 50 °C for 2 h and then boiled under reflux for 6 h. After the solution was concentrated to half the original volume, the resultant dark-purple crystals were collected by filtration, washed with ethanol and ether, and dried in vacuo. Yield: 66%. Anal. Calcd for C₄₂H₄₂BClF₄NiP₄: C, 59.23; H, 4.97; N, 0.00. Found: C, 59.18; H, 5.10; N, 0.00.

trans-[Pt(4-Cltp)₂{PdCl(pp₃)₂}(BF₄)₂] [**6**(BF₄)₂]. **1**(BF₄) (0.103 g, 0.103 mmol) and *trans*-[PtCl₂(NCC₆H₅)₂] (0.025 g, 0.052 mmol) were dissolved in acetonitrile (1 cm³). The reaction solution was concentrated by slow evaporation of the solvent to give yellow crystals. The crystals were collected by filtration and washed with ethanol. Yield: 76%. Anal. Calcd for C₉₆H₉₂B₂Cl₄F₈P₈Pd₂PtS₂·H₂O: C, 50.15; H, 4.12; N, 0.00. Found: C, 49.77; H, 4.11; N, 0.00. ¹⁹⁵Pt{¹H} NMR (CHCl₃): δ 38.64 (t, ¹J_{Pt–P} = 2767 Hz). The single crystals were obtained by recrystallization from chloroform.

trans-[PtCl₂{PdCl(pp₃)₂}(BF₄)₂] [**7a**(BF₄)₂]. To a solution of **2**(BF₄) (0.249 g, 0.277 mmol) in chloroform (10 cm³) was added *trans*-[PtCl₂(NCC₆H₅)₂] (0.064 g, 0.136 mmol) followed by filtration. Pale-yellow crystals were obtained by the addition of ethanol and water to the filtrate. Yield: 66%. Anal. Calcd for C₈₄H₈₄B₂Cl₄F₈P₈Pd₂Pt·H₂O: C, 48.44; H, 4.07; N, 0.00. Found: C, 48.40; H, 4.14; N, 0.00. The single crystals were obtained by recrystallization from chloroform.

cis-[PtCl₂{PdCl(pp₃)₂}Cl₂] (**7b**Cl₂). **2**Cl (0.194 g, 0.229 mmol) and *trans*-[PtCl₂(NCC₆H₅)₂] (0.054 g, 0.114 mmol) were dissolved in chloroform (1 cm³). The reaction mixture was allowed to stand at room temperature for 24 h to give pale-yellow crystals. The crystals were filtered and recrystallized from acetonitrile. Yield: 90%. Anal. Calcd for C₈₄H₈₄Cl₆P₈Pd₂Pt·CH₃CN·H₂O: C, 51.11; H, 4.44; N, 0.69. Found: C, 50.52; H, 4.40; N, 0.62. ¹⁹⁵Pt{¹H} NMR (CHCl₃): δ 289.29 (t, ¹J_{Pt–P} = 3690 Hz). The single crystals were obtained by recrystallization from acetonitrile.

trans-[PtCl₂{NiCl(pp₃)₂}(BF₄)₂] [**8**(BF₄)₂]. Dark-brown crystals were obtained by a procedure similar to that for **6**(BF₄)₂ using 0.099 g (0.12 mmol) of **5**(BF₄), 0.030 g (0.064 mmol) of *trans*-[PtCl₂(NCC₆H₅)₂], and 1.4 cm³ of acetonitrile. Yield: 60%. Anal. Calcd for C₈₄H₈₄B₂Cl₄F₈P₈Ni₂Pt·H₂O: C, 50.77; H, 4.36; N, 0.00. Found: C, 50.65; H, 4.36; N, 0.00.

- (2) (a) Nair, P.; Anderson, G. K.; Rath, N. P. *Inorg. Chem. Commun.* **2003**, 6, 1307. (b) Wachtler, H.; Schuh, W.; Ongania, K.-H.; Kopacka, H.; Wurst, K.; Peringer, P. *J. Chem. Soc., Dalton Trans.* **2002**, 2532. (c) Annibale, G.; Bergamini, P.; Bertolasi, V.; Besco, E.; Cattabriga, M.; Rossi, R. *Inorg. Chim. Acta* **2002**, 333, 116.
- (3) (a) Tsuji, J. *Palladium Reagents and Catalysts*; Wiley: Chichester, U.K., 1995. (b) Heck, R. F. *Palladium Reagents in Organic Synthesis*; VCH: Weinheim, Germany, 1996. (c) Beletskaya, I. P.; Chepravok, A. V. *Chem. Rev.* **2000**, 100, 3009.
- (4) Churchill, M. R.; Julis, S. A.; Rotella, F. J. *Inorg. Chem.* **1977**, 16, 1137.
- (5) Aizawa, S.; Iida, T.; Funahashi, S. *Inorg. Chem.* **1996**, 35, 5163.

- (6) King, R. B.; Kapoor, R. N.; Saran, M. S.; Kapoor, P. N. *Inorg. Chem.* **1971**, 10, 1851.
- (7) Hohman, W. H.; Kountz, D. J.; Meek, D. W. *Inorg. Chem.* **1986**, 25, 616.

Table 1. Crystallographic Data for **6**(BF₄)₂·2CHCl₃, **7a**(BF₄)₂·H₂O·CHCl₃, and **7b**Cl₂·H₂O·CH₃CN

	6 (BF ₄) ₂ ·2CHCl ₃	7a (BF ₄) ₂ ·H ₂ O·CHCl ₃	7b Cl ₂ ·H ₂ O·CH ₃ CN
formula	C ₉₈ H ₉₄ B ₂ Cl ₁₀ F ₈ P ₈ Pd ₂ PtS ₂	C ₈₅ H ₈₇ B ₂ Cl ₇ F ₈ OP ₈ Pd ₂ Pt	C ₉₂ H ₉₈ Cl ₆ N ₄ OP ₈ Pd ₂ Pt
fw	2519.76	2202.08	2144.21
cryst syst	triclinic	orthorhombic	monoclinic
space group	<i>P</i> $\bar{1}$	<i>Pbca</i>	<i>P</i> 2 ₁ / <i>c</i>
<i>a</i> , Å	15.510(2)	28.276(4)	20.121(6)
<i>b</i> , Å	15.854(3)	23.610(4)	27.80(1)
<i>c</i> , Å	22.923(3)	13.933(3)	18.758(5)
α , deg	97.53(1)		
β , deg	102.72(1)		114.06(2)
γ , deg	96.58(1)		
<i>V</i> , Å ³	5390(1)	9301(2)	9579(5)
<i>Z</i>	2	4	4
<i>D</i> _{calcd} , g cm ⁻³	1.552	1.572	1.487
μ , cm ⁻¹	2.082	2.275	2.169
<i>R</i> 1 ^a	0.050	0.075	0.052
<i>wR</i> 2 ^b	0.086	0.117	0.102

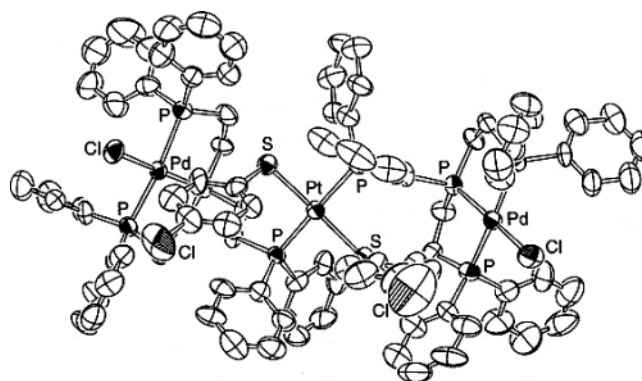
^a *R*1 = $\sum||F_o| - |F_c||/\sum|F_o|$. ^b *wR*2 = $[\sum w(F_o^2 - F_c^2)^2/\sum w(F_o^2)^2]^{1/2}$, where $w = 1/\sigma^2(F_o)^2$.

trans-[Pt(4-Cltp)₂{PdCl₂(pp₃)RhCl₂Cp*₂}]₂ (**9**). To a suspension containing **6**(BF₄) (0.084 g, 0.037 mmol) and [Rh₂Cl₂(μ -Cl)₂Cp*₂] (0.042 g, 0.068 mmol) in chloroform was gradually added a chloroform solution of Bu₄NCl (0.037 g, 0.133 mmol). This mixture was stirred at 30 °C for several minutes and then filtered. The filtrate was concentrated to ca. 3 cm³ followed by the addition of ethanol and a small amount of water to give pale-red crystals. Yield: 29%. Anal. Calcd for C₁₁₆H₁₂₂Cl₁₀P₈Pd₂PtRh₂S₂·2CHCl₃: C, 46.70; H, 4.12; N, 0.00. Found: C, 46.80; H, 4.34; N, 0.00.

trans-[PtCl₂{PdCl₂(pp₃)RhCl₂Cp*₂}]₂ (**10a**). Pale-red crystals of **10a** were obtained by a procedure similar to that of **9** using 0.084 g (0.040 mmol) of **7a**(BF₄)₂, 0.045 (0.073 mmol) of [Rh₂Cl₂(μ -Cl)₂Cp*₂], and 0.041 g (0.15 mmol) of Bu₄NCl. Yield: 55%. Anal. Calcd for C₁₀₄H₁₁₄Cl₁₀P₈Pd₂PtRh₂·H₂O: C, 48.08; H, 4.50; N, 0.00. Found: C, 47.99; H, 4.48; N, 0.00.

cis-[PtCl₂{PdCl₂(pp₃)RhCl₂Cp*₂}]₂ (**10b**). **7b**Cl₂ (0.029 g, 0.015 mmol) and [Rh₂Cl₂(μ -Cl)₂Cp*₂] (0.010 g, 0.017 mmol) were dissolved in chloroform (10 cm³) at 30 °C. To the resultant red solution was added diethyl ether, and the mixture was kept in a refrigerator to give pale-red crystals. Yield: 55%. Anal. Calcd for C₁₀₄H₁₁₄Cl₁₀P₈Pd₂PtRh₂·2H₂O: C, 47.86; H, 4.56; N, 0.00. Found: C, 47.48; H, 4.36; N, 0.00.

X-ray Structural Determinations. The crystal and molecular structures of **6**(BF₄)₂, **7a**(BF₄)₂, and **7b**Cl₂ have been determined by X-ray diffraction methods (Table 1). Each crystal was sealed in a Lindemann glass-capillary tube with the mother liquor. Intensity data of **6**(BF₄)₂ and **7a**(BF₄)₂ were collected on a Rigaku AFC-5R diffractometer using Mo K α radiation (0.710 73 Å) in ω -2 θ and ω scan modes, respectively, and those of **7b**Cl₂ were collected on a Rigaku AFC-7R diffractometer in the ω scan mode. All data were corrected for Lorentz and polarization effects, and an absorption correction based on ψ scans was applied for **7a**(BF₄)₂ and **7b**Cl₂. The structures were solved using direct methods⁸ and refined by full-matrix least-squares procedures on *F*² using the CrystalStructure program.^{9–11} All non-hydrogen atoms were refined anisotropically, and all of the hydrogen atoms were refined using a riding method.

**Figure 1.** ORTEP diagram of a complex cation of **6**.

Measurements. ¹⁹⁵Pt, ³¹P, and ¹H NMR spectra were recorded on a JEOL JNM-A400 FT-NMR spectrometer operating at 85.48, 160.70, and 399.65 MHz, respectively. To determine the chemical shifts of ¹⁹⁵Pt and ³¹P NMR signals, a 3-mm-o.d. NMR tube containing the sample solution was coaxially mounted in a 5-mm-o.d. NMR tube containing deuterated water as a lock solvent and K₂[Pt(CN)₄] and phosphoric acid as references, respectively. The crystallizing solvents in the crystals were confirmed by ¹H NMR. UV–vis absorption spectra were recorded on a Perkin-Elmer Lambda 19 spectrophotometer.

General Procedure for the C–C Coupling Reaction. Reactions of iodobenzene (28.2 mmol) with styrene (42.2 mmol) in *N,N*-dimethylformamide (3 cm³) were carried out under nitrogen at 125 °C in the presence of tributylamine (75 mmol) as a base and the mononuclear or polynuclear complexes (0.035 mmol for **2Cl**, **3Cl**, and **4**; 0.017 mmol for **7a**(BF₄)₂, **7b**Cl₂, **10a**, and **10b**) as catalysts. The yields were calculated by the ¹H NMR intensity of the ortho protons of *trans*-stilbene formed on the basis of the intensity of the ethylene protons of bis(2-butoxyethyl) ether contained as an internal reference and followed as a function of time.

Results and Discussion

Structure of Complexes. The linear trinuclear structures with alternate metal arrangements of Pd(II)–Pt(II)–Pd(II) for **6**(BF₄)₂, **7a**(BF₄)₂, and **7b**Cl₂ were confirmed by X-ray analyses (Figures 1–3). The crystal structures revealed that the thiolato ligand in [Pd(4-Cltp)(pp₃)](BF₄) and chloro ligands in *trans*-[PtCl₂(NCC₆H₅)₂] were exchanged in the trinuclear complex **6** and the geometry of *trans*-[PtCl₂(NCC₆H₅)₂] was changed to *cis* geometry on the Pt(II) center

- (8) Sheldrick, G. M. *SHELXS-86*; University of Göttingen: Göttingen, Germany, 1986. Sheldrick, G. M. *SHELXS-97*; University of Göttingen: Göttingen, Germany, 1997.
- (9) CrystalStructure 3.5.1; Crystal Structure Analysis Package, Rigaku and Rigaku/MS, 2000–2003.
- (10) Watkin, D. J.; Prout, C. K.; Carruthers, J. R.; Betteridge, P. W. *CRYSTALS*, Issue 10; Chemical Crystallography Laboratory: Oxford, U.K., 1996.
- (11) Though full-matrix least-squares refinements for **7a** were carried out considering the disorder of the phenyl group, the result was not improved with any occupancy factors.

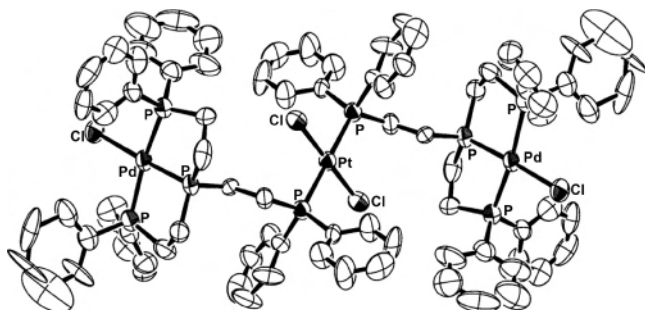


Figure 2. ORTEP diagram of a complex cation of **7a**.

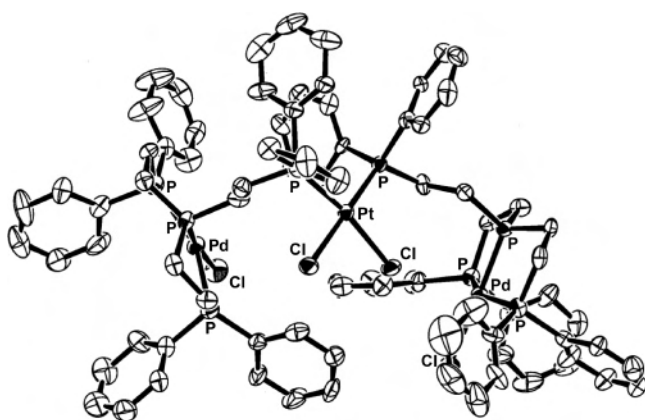


Figure 3. ORTEP diagram of a complex cation of **7b**.

Table 2. Average Bond Distances (Å) and Angles (deg) for the Trinuclear Complexes

	6	7a	7b
Pt–Pt ^a	2.300	2.329	2.252
Pt–S	2.344		
Pt–Cl		2.286	2.350
Pd–P _c ^a	2.223	2.210	2.216
Pd–P _t ^a	2.328	2.341	2.320
Pd–Cl	2.368	2.363	2.357
P _t –Pt–P _t ^a	174.6	180.0	98.0
P _t –Pt–Cl ^a			172.8
S–Pt–S	175.4		
Cl–Pt–Cl		180.0	86.8
P _t –Pd–P _t ^a	159.3	166.4	155.6
P _c –Pd–Cl ^a	175.3	176.8	174.5

^a P_t and P_c denote the terminal and central P atoms of the pp₃ ligand.

in **7b**, while the trans geometry was retained in **7a**. As shown in Table 2, the structures of the terminal Pd(II) moieties are almost the same, having similar average bond distances for the central and terminal phosphino groups of the pp₃ ligand (Pd–P_c = 2.210–2.223 Å and Pd–P_t = 2.320–2.341 Å, respectively) and the chloro ligands (Pd–Cl = 2.357–2.368 Å), whereas the bond distances around the Pt(II) center change appreciably depending on its geometry; namely, the average Pt–P distances for **6** (2.300 Å) and **7a** (2.329 Å) are obviously longer than that for **7b** (2.252 Å), and the average Pt–Cl distance (2.350 Å) for **7b** is elongated compared with **7a** (2.286 Å) because of the trans influence of the P atoms. Furthermore, it is apparent that the square-planar structure of the Pd(II) moieties is highly distorted by the chelate strain of the pp₃ ligand compared with that of the Pt(II) center; that is, the average P_t–Pd–P_t bond angles for **6**, **7a**, and **7b** (155.6–166.4°) deviate from 180°

appreciably, while the P_t–Pt–P_t angles for **6** and **7a** and the P_t–Pt–Cl (trans) angles for **7b** are within the normal range (172.8–180.0°) (Table 2). Such a distortion by the pp₃ ligand, which acts as a tridentate ligand in the Pd(II) terminals, was similarly observed for the square-planar Pd(II) complexes with the linear tridentate p₃¹² and pp₃O¹ ligands.

The ³¹P NMR spectra of the trinuclear complexes **6**, **7a**, and **7b** in chloroform are consistent with their crystal structures. By comparison with the ³¹P NMR spectra of [Pd(4-Cltp)(pp₃O)]¹ (Table 3), the signals in the ranges of 114.4–118.4 ppm and 46.0–47.2 ppm coupled with each other (³J_{P–P} = 7.3–7.6 Hz) are reasonably assigned to those for the central and two terminal P atoms of pp₃ coordinated to the square-planar Pd(II) ion, respectively. The other signals (12.2–14.3 ppm) with a pair of satellite peaks due to ¹⁹⁵Pt (¹J_{P–Pt} = 2580–3690 Hz) coupled with the central P atom (³J_{P–P} = 44–55 Hz) are assigned to the terminal P atoms bridging to the Pt(II) center. The triplets of ¹⁹⁵Pt NMR for **6** and **7b** (see the Experimental Section), which show the coupling constants equal to the respective ¹J_{P–Pt} values obtained by ³¹P NMR, indicate that the two equivalent terminal P atoms are coordinated to the Pt(II) center. Because the AA'XX' spin system is made up of the two chemically equivalent terminal P atoms (A and A') bridging to the Pt(II) center and the two central P atoms (X and X') in the Pd(II) moieties, the virtual ²J_{P–P} coupling through the Pt(II) center can be observed. In fact, the ³¹P NMR spectral simulations¹³ for the bridging P atoms (Figure 4) revealed large differences in the ²J_{P–P} values attributed to the difference in geometry around the Pt(II) center; that is, the considerably large ²J_{P–P} values were observed for the trans isomers, **6** (500 Hz) and **7a** (400 Hz), and the relatively small values for the cis isomer, **7b** (13 Hz) (Figure 4 and Table 3). Furthermore, the relatively large ¹J_{P–Pt} value for **7b** (3690 Hz) compared with those for **6** (2767 Hz) and **7a** (2580 Hz) corresponds to the shorter Pt–P bond distances for **7b** than those for **6** and **7a** observed in the crystal structures. The ³¹P NMR signals for **8**, which was prepared by the reaction of *trans*-[PtCl₂(NCC₆H₅)₂] and the trigonal-bipyramidal Ni(II) complex **5**(BF₄) instead of **2**(BF₄), are consistent with the phosphine-bridged trinuclear structure with the terminal and central P atoms on the square-planar Ni(II) ions and the other terminal P atoms bridging to the Pt(II) center. The spectral pattern showing the strong coupling through the Pt(II) center (²J_{P–P} = 580 Hz) and the relatively small value of ¹J_{P–Pt} (2555 Hz) similar to those for **6** and **7a** indicates the retention of the trans geometry around the Pt(II) center.

The ³¹P NMR spectrum of **9** in chloroform exhibits four signals corresponding to the four P atoms of the pp₃ ligand, as shown in Figure 5. Multiplets at 88.6 and 89.5 ppm and doublets at 68.1 and 68.5 ppm coupled with each other (³J_{P–P} = 12 Hz) can be assigned to the central and terminal P atoms on the square-planar Pd(II) ions by comparison with the ³¹P NMR spectrum of [Pd(4-Cltp)₂(pp₃O₂)].¹ Signals at 14.3 and

(12) Aizawa, S.; Sone, Y.; Kawamoto, T.; Yamada, S.; Nakamura, M. *Inorg. Chim. Acta*, **2002**, *338*, 235.

(13) *gNMR*, version 5.0; Adept Scientific plc: Herts, U.K., 2003.

Table 3. ^{31}P NMR Data for Trinuclear and Pentanuclear Complexes

		$[\text{Pd}(4\text{-Cltp})^- (\text{pp}_3\text{O})]^+{}^a$	6	7a	7b	8	9	10a	10b
$\text{P}_t\text{-Pt}^b$	δ		14.3 (t, 2P)	14.0 (t, 2P)	12.2 (dt, 2P)	14.0 (t, 2P)	14.3, 14.7 (t, 2P)	13.4, 13.7 (t, 2P)	9.8, 10.1 (dt, 2P)
	$^1J_{\text{P-Pt}}$		2767	2580	3690	2555	2647	2531	3657
	$^2J_{\text{P-P}}$		500	400	13	580	550	365	13
	$^3J_{\text{P-P}}$		55	44	48	45	49	44	52
P=O^c	δ	32.3 (d, P)							
	$^3J_{\text{P-P}}$	33							
$\text{P}_t\text{-Pd}^d$	δ		47.6 (d, 2P)	46.7 (d, 4P)	46.0 (d, 4P)	47.7 (d, 4P)	68.1, 68.5 (d, 2P)	68.4, 68.5 (d, 2P)	68.8, 69.1 (d, 2P)
	$^3J_{\text{P-P}}$		16.5	7.3	7.4	44.3	12	12	14
$\text{P}_c\text{-Pd}^e$	δ	107.0 (dt, P)	118.4 (m, 2P)	115.6 (m, 2P)	114.4 (m, 2P)	115.9 (m, 2P)	88.6, 89.5 (m, 2P)	89.3 (m, 2P)	88.8 (m, 2P)
$\text{P}_t\text{-Rh}^f$	δ						27.6, 27.7 (dd, 2P)	27.8 (dd, 2P)	27.9 (dd, 2P)
	$^1J_{\text{P-Rh}}$						144	145	144
	$^3J_{\text{P-P}}$						54	55	52

^a Reference 1. ^b Terminal P atom bridging to the Pt(II) center. ^c Oxidized P atom. ^d Terminal P atom in the Pd(II) moiety. ^e Central P atom in the Pd(II) moiety. ^f Terminal P atom bridging to the Rh(III) terminal.

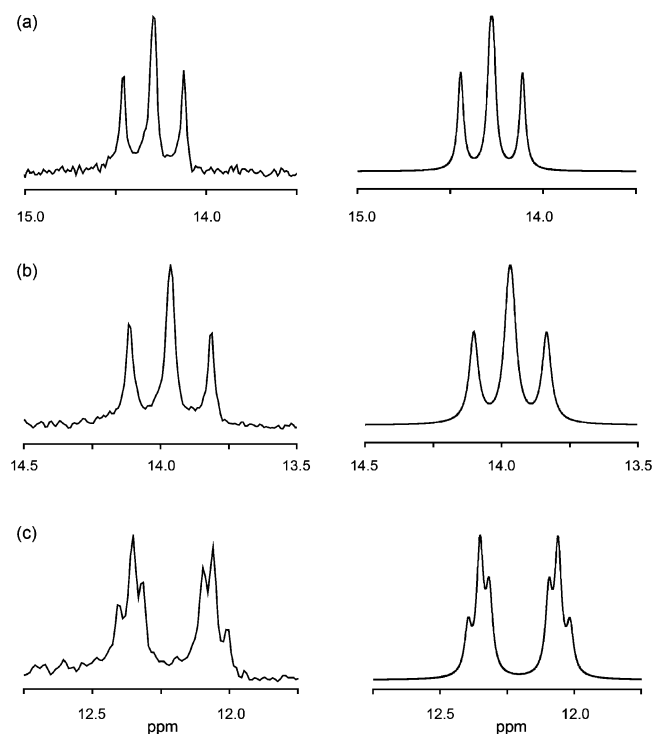


Figure 4. Observed (left) and simulated (right) ^{31}P NMR spectra for the bridging P atoms of **6** (a), **7a** (b), and **7b** (c). The simulated spectra are depicted by using $^2J_{\text{P-P}} = 500$ Hz and $^3J_{\text{P-P}} = 55$ Hz for **6**, $^2J_{\text{P-P}} = 400$ Hz and $^3J_{\text{P-P}} = 44$ Hz for **7a**, and $^2J_{\text{P-P}} = 13$ Hz and $^3J_{\text{P-P}} = 48$ Hz for **7b**.

14.7 ppm showing coupling with ^{195}Pt ($^1J_{\text{P-Pt}} = 2647$ Hz) and the central P atom ($^3J_{\text{P-P}} = 49$ Hz) are assigned to the terminal P atoms bridging to the Pt(II) center. The NMR spectral simulation¹³ determined the large coupling constant ($^2J_{\text{P-P}} = 550$ Hz) between the two equivalent terminal P atoms through the Pt(II) center as obtained for **6**, consistent with the trans geometry around the Pt(II) square plane. Agreements of the ^{31}P NMR chemical shifts for the terminal P atoms on the Pt(II) center and the AB splitting pattern of ^1H NMR for the bound 4-Cltp⁻ ligands between **6** (δ 6.28 and 6.67, $^3J_{\text{H-H}} = 9$ Hz) and **9** (δ 6.37 and 6.55, $^3J_{\text{H-H}} = 9$ Hz) indicate the same trans thiolato structure of the Pt(II) centers. The other signals at 27.6 and 27.7 ppm coupled with ^{103}Rh ($^1J_{\text{P-Rh}} = 144$ Hz) and the central P atom ($^3J_{\text{P-P}} = 54$ Hz) are assigned to the terminal P atoms bound to the Rh-

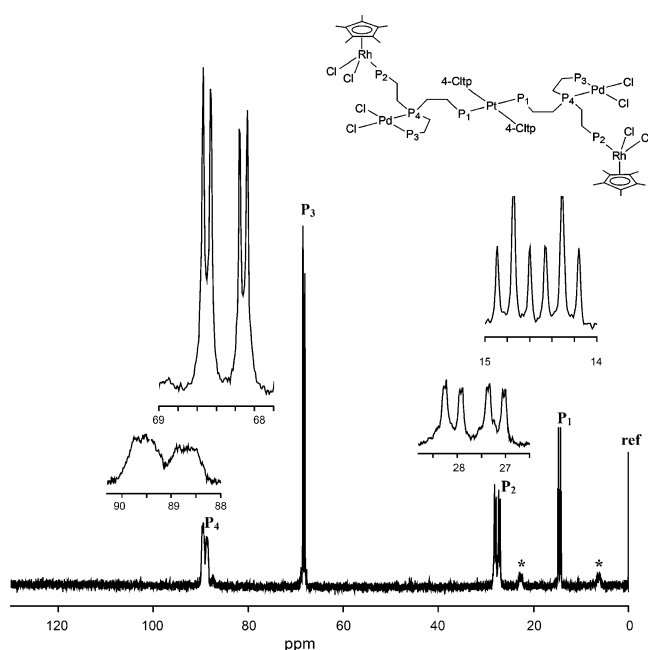


Figure 5. ^{31}P NMR spectrum of **9** in chloroform. Asterisks and ref denote satellite peaks due to ^{195}Pt and the signal for D_3PO_4 in the outer D_2O , respectively.

(III) terminals by comparison with the reported ^{31}P NMR chemical shifts and $^1J_{\text{P-Rh}}$ values for the Rh(III) complexes having $[\text{RhCl}_2\text{Cp}^*\text{L}]$ (L = diphenylphosphino group) moieties with a three-legged piano-stool structure.¹⁴ The ^1H NMR chemical shift (1.34 ppm) and $^2J_{\text{H-Rh}}$ value (3.2 Hz) for the bound Cp^* are also in good agreement with those for the $[\text{RhCl}_2\text{Cp}^*\text{L}]$ moieties.¹⁴ Two sets of the four ^{31}P NMR signals correspond to formation of the meso and racemic isomers by combination of the two chiral central P atoms in the two Pd(II) moieties. The above NMR spectral behaviors unquestionably indicate that **9** has the Rh(III)-Pd(II)-Pt(II)-Pd(II)-Rh(III) pentanuclear structure with trans geometry of the Pt(II) center and the three-legged piano-stool structure of the terminal Rh(III) moieties linked by the pp_3 ligands on the square-planar Pd(II) ions. The structural assignments for **10a** and **10b** were carried out similarly by the ^{31}P NMR spectra though the ^{31}P NMR signals for meso

(14) Stoppioni, P.; Vaira, M. D.; Maitlis, P. M. *J. Chem. Soc., Dalton Trans.* **1982**, 1147.

and racemic isomers are overlapped in the regions of the central P atoms in the Pd(II) moieties and the terminal P atoms in the terminal Rh(III) moieties. The trans and cis geometries of the Pt(II) centers for **10a** and **10b** were demonstrated by the large difference in the ^{31}P NMR coupling through the Pt(II) center ($^2J_{\text{P-P}} = 365$ Hz for **10a** and 13 Hz for **10b**) and the difference in the $^1J_{\text{P-Pt}}$ value (2531 Hz for **10a** and 3657 Hz for **10b**) similarly to the geometries for **7a** and **7b**. These facts indicate that the bridging reactions of the trinuclear Pd(II)–Pt(II)–Pd(II) complexes with $[\text{Rh}_2\text{Cl}_2(\mu\text{-Cl})_2\text{Cp}^*_2]$ successfully proceed to give the pentanuclear structure retaining the geometries around the Pt(II) center and the three-legged piano-stool Rh(III) structure.

Bridging Reaction. We have previously reported the selective oxidation of the terminal P atom of the pp_3 ligand in the equatorial position of **1**(BF_4) in acetonitrile and chloroform and have expected the formation of the square-planar intermediate with one dissociated pendant phosphino group even in the inert solvent (**I**₁ in Scheme 1).¹ From the fact that further oxidation of another terminal P atom proceeds quantitatively by the addition of excess 4-Cltp[−], it is probable that the terminal P atom of $[\text{Pd}(4\text{-Cltp})(\text{pp}_3\text{O})]^+$ is dissociated by the substitution reaction with 4-Cltp[−] to form the intermediate **I**₂ in Scheme 1, while the P atoms of the bidentate pp_3O_2 ligand in $[\text{Pd}(4\text{-Cltp})_2(\text{pp}_3\text{O}_2)]$ are hardly dissociated.¹ In the present work, we have attempted to employ the dissociated phosphino groups in the respective intermediates as linking groups for the stepwise bridging reactions to the Pt(II) and Rh(III) ions, expecting that the chloride counteranion of **7b** and the chloride anion added in the preparations for **9** and **10a** play the same role as 4-Cltp[−] used for the second oxidation step. In fact, the reaction solutions for the preparation of the mixed-metal polynuclear complexes, **6**(BF_4)₂, **7a**(BF_4)₂, **7b**Cl₂, **8**(BF_4)₂, **9**, **10a**, and **10b**, exhibit ^{31}P NMR spectra coinciding with those of the corresponding isolated complexes with little impurity. Furthermore, the ^{31}P NMR spectra of the isolated complexes in chloroform were not changed at room temperature at least for several days. These facts indicate that the above polynuclear complexes with intended metal-ion sequences were formed quantitatively and the isolated complexes are stable in the inert solvent. In other words, the enthalpy loss by the Pd(II)–P bond dissociation and the entropic energy loss by the phosphine bridging are sufficiently compensated for by the enthalpy gain for the Pt(II)–P or Rh(III)–P bond formation.

The cis isomer of the Ni(II)–Pt(II)–Ni(II) trinuclear complex and the Rh(III)–Ni(II)–Pt(II)–Ni(II)–Rh(III) pentanuclear complex could not be obtained by a procedure similar to that for **7b**Cl₂ by using **5**Cl instead of **2**Cl and that for **10a** by using **8**(BF_4)₂ instead of **7a**(BF_4)₂, respectively, because the phosphine transfer reaction from Ni(II) onto Pt(II) proceeded to give $[\text{PtCl}(\text{pp}_3)]\text{Cl}$.¹⁵ Considering that the trinuclear complex **8**(BF_4)₂ was formed quantitatively and was stable in chloroform in the absence of the free

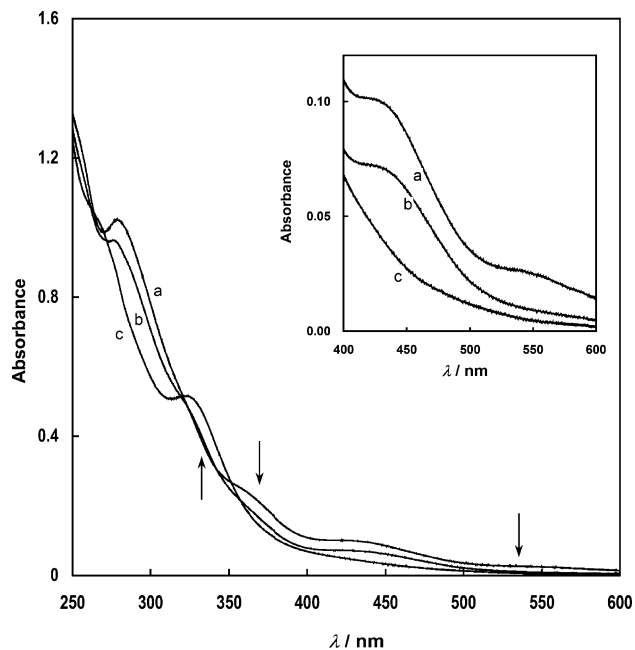


Figure 6. Absorption spectra of a chloroform solution containing **1** (2.3×10^{-5} mol kg^{−1}) and *trans*- $[\text{PtCl}_2(\text{NCC}_6\text{H}_5)_2]$ (1.0×10^{-5} mol kg^{−1}) at 30 s (a), 3600 s (b), and 32400 s (c) after the reaction started. The direction of the spectral change is denoted by arrows, and the inset shows the spectral change in the d–d absorption region for the five-coordinate trigonal-bipyramidal Pd(II) complexes.

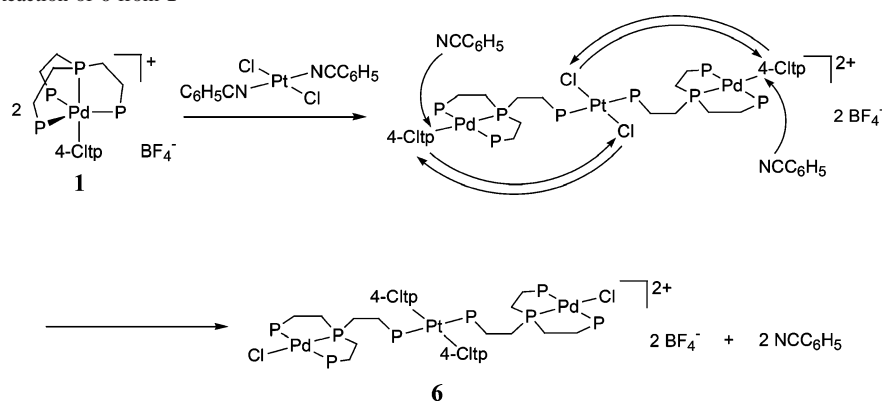
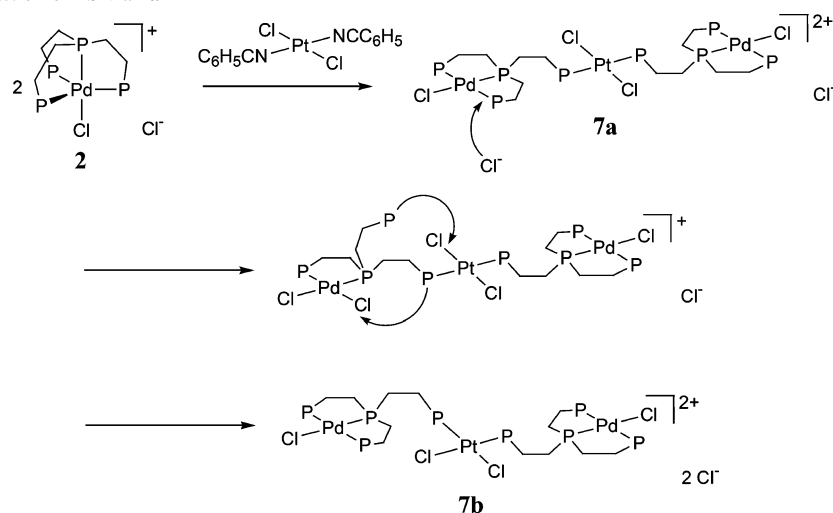
chloride ion, the Ni(II)–P bonds were broken by coordination of the chloride ion. Such a difference in reactivity between Pd(II) and Ni(II) is attributed to a difference in the relative bond strength for the coordinated P atoms.

Structural Conversion. Considering the structures of the final products, additional transformations besides the phosphine bridging were required for the formation of **6** and **7b** where the exchange between the thiolato ligand on Pd(II) and the chloro ligands on Pt(II) proceeded for **6** and the trans-to-cis geometrical change on the Pt(II) center proceeded for **7b**.

The absorption spectral change during the formation reaction of **6** indicated two-step successive reactions where the isosbestic points shifted from 262, 325, and 343 nm to 260, 271, 320, and 357 nm. The lower energy d–d absorption band ($^1A_1' \rightarrow ^1E'$) at around 550 nm characteristic of the five-coordinate trigonal-bipyramidal Pd(II) complexes^{5,16} disappeared in the first step and the shoulder at around 440 nm assignable to the d–d absorption band for the square-planar $[\text{palladium}(\text{thiolato})(\text{phosphine})_3]$ chromophore¹² disappeared in the second step (Figure 6). This spectral behavior suggests that the bridging of the terminal P of the pp_3 ligand in **1** proceeded initially and the monodentate ligands, 4-Cltp[−] on the Pd(II) ion and Cl[−] on the Pt(II) ion, were exchanged subsequently. This mechanism was confirmed by a change in the ^{31}P and ^1H NMR spectra where the NMR signals of the bound pp_3 and 4-Cltp[−] ligands for the initially formed trinuclear complex¹⁷ decreased and those for the final product **6** increased gradually. Benzonitrile dissociated from Pt(II) by the initial phosphine-bridging reaction probably acts as

(15) Fernández, D.; Seijo, M. I. G.; Kégl, T.; Petőcz, G.; Kollár, L.; Fernández, M. E. G. *Inorg. Chem.* **2002**, *41*, 4435.

(16) Lever, A. B. P. *Inorganic Electronic Spectroscopy*, 2nd ed.; Elsevier: Amsterdam, The Netherlands, 1984; Chapter 6.

Scheme 2. Formation Reaction of **6** from **1**Scheme 3. Formation Reaction of **7b** via **7a**

the attacking ligand that is required for the associative substitution reaction of the four-coordinate square-planar d^8 metal complexes¹⁸ (Scheme 2). Furthermore, this fact justified the two-term rate law, $k = k_1 + k_2[\text{entering ligand}]$, with the solvolysis path k_1 , where k_2 is the rate constant for the direct ligand substitution path, which has been proposed on the basis of the kinetic results for the ligand substitution of the square-planar Pd(II) and Pt(II) complexes.^{18,19} From a thermodynamic point of view, this exchange reaction demonstrates that the difference in the affinities for the thiolato S atom between Pt(II) and Pd(II) is much greater than that for the chloro ligand. The retention of the trans geometry around Pt(II) during the ligand exchange indicates that the total trans influence between the S and P atoms on the square-planar Pt(II) ion exceeds the total of the trans influence between the S atoms and that between the P atoms in **6**, considering that little difference in the steric crowding can be found between the trans and cis geometries.

The reaction solution for the preparation of **7b** by using **2Cl** exhibited the ³¹P NMR signals of **7a** initially, and the

isomerization proceeded gradually to give **7b** quantitatively in several hours. The isomerization of **7a** to **7b** was also completed by the addition of 1 equiv of Bu₄NCl to a chloroform solution of **7a**(BF₄)₂. In contrast, the trans-to-cis isomerizations of the pentanuclear complex **10a** did not proceed in the presence of excess Bu₄NCl (see the Experimental Section). Such a difference in the isomerization behavior between the trinuclear and pentanuclear complexes indicates that the geometrical change is initiated by an attack of the outer Cl⁻ onto the terminal Pd(II) moiety followed by the dissociation of the terminal phosphino group of the pp₃ ligand acting as tridentate in the Pd(II) terminal. The terminal phosphino group of the pp₃ ligand acting as bidentate in the Pd(II) moieties in the pentanuclear complex **10b** is hardly dissociated by the outer attacking ligands, considering that the further oxidation of [Pd(4-Cltp)(pp₃O₂)] (Scheme 1) did not proceed in the presence of excess 4-Cltp⁻.¹ Such a high reactivity of the tridentate pp₃ ligand on Pd(II) compared with the bidentate pp₃ one is attributed to the trans effect between the terminal P atoms and the chelate strain of the tridentate pp₃ ligand as observed in the crystal structures in **6**, **7a**, **7b**, and [Pd(4-Cltp)(pp₃O)]⁺.¹ The dissociated terminal phosphino group of the pp₃ ligand can replace the bridging terminal phosphino group of the same pp₃ ligand on the Pt(II) center with the geometrical change (Scheme 3). The above isomerization behavior of the trinuclear complex demonstrates that kinetically stable **7a**

(17) ³¹P{¹H} NMR (CHCl₃): δ 13.7 (t, 2P, ¹J_{P-Pt} = 2570 Hz, ²J_{P-P} = 450 Hz, ³J_{P-P} = 44 Hz), 47.8 (d, 4P, ³J_{P-P} = 16.7 Hz), 109.8 (tt, 2P). ¹H NMR (CHCl₃): δ 6.72, 6.51 (AB system, ³J_{H-H} = 8 Hz).

(18) Wilkins, R. W. *Kinetics and Mechanism of Reaction of Transition Metal Complexes*, 2nd ed.; VCH: Weinheim, Germany, 1991; Chapter 4. (b) Cross, R. J.; Twigg, M. V. *Mechanisms of Inorganic and Organometallic Reactions*; Plenum: New York, 1988; Chapter 5. (c) Lin, Z.; Hall, M. B. *Inorg. Chem.* **1991**, *30*, 646.

(19) Gray, H. B. *J. Am. Chem. Soc.* **1962**, *84*, 1548.

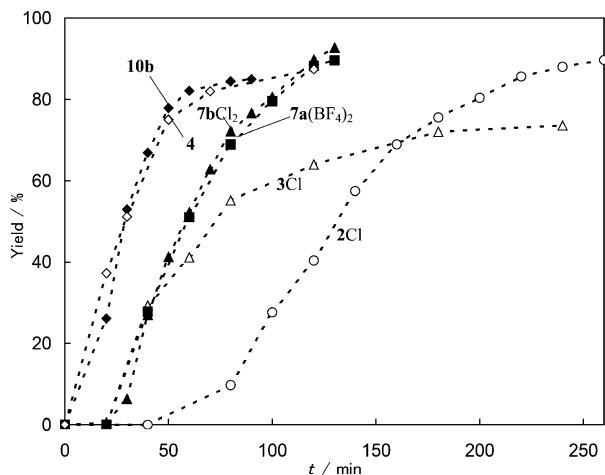


Figure 7. Changes in the yield of stilbene with time in Heck reactions catalyzed by **2Cl**, **3Cl**, **4**, **7a(BF₄)₂**, **7bCl₂**, and **10b**.

in the absence of the entering ligand was converted into the thermodynamically more stable isomer **7b**, avoiding the trans influence between the P atoms on the Pt(II) center. It is noteworthy that the trans and cis isomers of the trinuclear and pentanuclear complexes are formed quantitatively and prepared selectively simply by changing the counteranion of the starting Pd(II) complexes.

C–C Coupling Reaction. It is important to confirm whether the bridging structures of the mixed-metal complexes are maintained in the employed reaction system in order to investigate cooperative effects of the different metal ions. We adopted the Heck-type C–C coupling reaction^{3b,c} that is one of the most widespread Pd-catalyzed reactions. Because it is difficult to observe the transient structures of catalytically active species under the usual conditions of the catalytic reactions, we intended to obtain some structural information about the active species from differences in catalytic activity.

The catalytic activities of the chloro mononuclear (**2Cl**), trinuclear [**7a(BF₄)₂** and **7bCl₂**], and pentanuclear (**10b**) complexes were compared to one another using iodobenzene and styrene as the substrates under the same conditions in which the concentrations of the catalysts were normalized by using the concentrations of Pd(II) (see the Experimental Section). Furthermore, the catalytic activities of the mononuclear complexes with the tridentate p₃ ligand (**3Cl**) and the bidentate p₂ ligand (**4**) are also compared with those of **7a(BF₄)₂**, **7bCl₂**, and **10b** because the pp₃ ligands in the Pd(II) moieties act as tridentate in **7a(BF₄)₂** and **7bCl₂** and

bidentate in **10b**. Shortening of the induction period and acceleration of the reaction were the following order: mononuclear **2Cl** < mononuclear **3Cl** < trinuclear **7a(BF₄)₂** and **7bCl₂** < pentanuclear **9b** and mononuclear **4** (Figure 7), depending on the number of bound P atoms on the Pd(II) ions (four for **2**, three for **3**, **7a**, and **7b**, and two for **4** and **9b**) but not on their polynuclear structures, geometries around Pt(II), or counterions. Considering that the ease of the prereduction and the subsequent oxidative addition of the substrates depend on the coordination environment around Pd(II),³ it is probable that the phosphine bridging to the relatively inert metal ions, Pt(II) and Rh(III), is not broken in the catalytic reaction, maintaining the numbers of the phosphino groups that can be coordinated to Pd(II). On the other hand, better retention of the catalytic activity for the trinuclear complexes **7a(BF₄)₂** and **7bCl₂** compared with the mononuclear complex **3Cl** may be attributed to the effect of the neighboring Pt(II) ion. Recently, we reported the rapid equilibrium of the Pt(II) complex with the pp₃ ligand between the five-coordinate trigonal-bipyramidal geometry and the five-coordinate square-pyramidal one with an iodide ion in the apical position, [Pt(pt)(pp₃)]⁺ + I[−] ⇌ [PtI(pt)(pp₃)] (pt = 1-propanethiolate).²⁰ This result suggests that the five-coordinate structures of Pt(II) complexes are considerably stabilized by the soft P donors. Because at least one of the three bound P atoms on the Pd(II) ion in **3Cl**, **7a(BF₄)₂**, and **7bCl₂** needs to be dissociated during the process from the oxidative addition of aryl halide to the reductive elimination of the coupled product,³ it is possible that the Pt(II) center in the trinuclear complexes attaches the dissociated phosphino group in the apical position in the catalytic cycle. Such an interaction between the Pt(II) ion and the P atom may assist the acceleration of the catalytic reaction and protect the dissociated phosphino group against oxidation not to form phosphine oxide. This can be regarded as one of the cooperative effects of the bridged metal ion.

Supporting Information Available: X-ray crystallographic information including final atomic coordinates, anisotropic thermal parameters, and full bond lengths and angles in CIF format. This material is available free of charge via the Internet at <http://pubs.ac.org>.

IC060277L

(20) Aizawa, S.; Kobayashi, T.; Kawamoto, T. *Inorg. Chim. Acta* **2005**, *358*, 2319.